

NUMERICAL MODELING OF THE AERODYNAMICS, HEAT EXCHANGE, AND COMBUSTION OF A POLYDISPERSE ENSEMBLE OF COKE-ASH PARTICLES IN ASCENDING AXISYMMETRIC TWO-PHASE FLOW

B. B. Rokhman

UDC 532.529:532.517.4

A two-dimensional stationary model of motion, heat and mass exchange, and chemical reaction of polydisperse coke and ash particles in ascending gas-suspension flow has been constructed with allowance for the turbulent and pseudoturbulent mechanisms of transfer in the dispersed phase. The system of equations that describes motion and heat transfer in the solid phase has been closed at the level of the equations for the second moments of velocity and temperature pulsations, whereas the momentum equations of the carrying medium have been closed using the equation for turbulent gas energy, which allows for the influence of the particles and heterogeneous reactions.

Keywords: combustion, particle, gas, polydispersity, turbulence, pseudoturbulence, temperature, pulsations, heterogeneous reaction, concentration, velocity, moments, aerodynamics.

Introduction. Development of the methods of mathematical modeling of transfer processes related to the burning of polyfractional solid fuel in combustion chambers is of great practical interest. The main difficulties of construction of this class of models are associated with the influence of polydispersity and turbulent and pseudoturbulent (random motion of the dispersed phase due to interparticle collisions) transfer mechanisms on the processes of aerodynamics, heat and mass exchange, and combustion in such devices. In [1], we have investigated the influence of the effect of interparticle interaction on the parameters of physicochemical processes in the combustion of anthracite culm in the ascending highly-concentrated polydisperse flow. It has been shown that the averaged interfractional-interaction force contributes to the equalization of the velocities of large and small coke-ash particles, because of which the degree of conversion of large fractions becomes noticeably lower. In [2–4], we have constructed a two-dimensional model of the motion, heat exchange, and combustion of a polydisperse ensemble of coke and ash particles with allowance for the turbulent and pseudoturbulent effects in the isotropic energy field of random motion of the solid phase. It has been shown that the pulsation energy of the particles is much higher than the turbulent energy of the gas. The dominant role of the pseudoturbulent mechanism of transfer in nonisothermal chemically reacting highly-concentrated polydisperse flows has been inferred.

Formulation of the Problem. In the present work, we propose a mathematical model constructed with the equations of transfer of the averaged and pulsation (velocity and temperature fluctuations) parameters of the dispersed phase with allowance for the radiant and convective heat exchange, heterogeneous reactions, interphase- and interparticle-interaction forces, and turbulent and pseudoturbulent effects for calculation of ascending axisymmetric nonisothermal flow of a polydisperse coke-ash mixture within the framework of the so-called two-liquid models (Eulerian approximation). The equations of motion of the carrying medium are closed on the basis of a one-parameter turbulence model generalized to the case of nonisothermal two-phase turbulent flows with chemical reaction.

In constructing the model, we start from the following simplifying prerequisites: 1) we consider the process as stationary; 2) we consider a two-phase heterogeneous medium consisting of the carrying medium — nitrogen, oxygen, and carbon dioxide — and the solid phase, which is presented in the form of two ensembles (coke+ash) of the finite number of monodisperse fractions M_C and M_{ash} each); 3) the stoichiometric reaction scheme includes the heterogeneous reaction $C + O_2 = CO_2$ that proceeds on the exterior surface of impermeable spherical particles; 4) we use the

boundary-layer approximation: $v \ll u$, $u' \ll u$, $v' \sim v$, and $\frac{\partial}{\partial z} \ll \frac{\partial}{\partial r}$; 5) we disregard change in the gas pressure in the cross section of the flow.

With allowance for what has been said above, a system of the averaged equations of mass, momentum, and energy transfer in the two-phase medium in the approximation of a narrow channel has the following form:

1. The continuity equations for the components of the carrying medium are

$$\frac{\partial (C_{O_2} u_g)}{\partial z} + \frac{\partial [r (C_{O_2} v_g + \langle C'_{O_2} v'_g \rangle)]}{r \partial r} = -6 \sum_{j=1}^{M_C} \frac{L_j S_j \beta_j C_{O_2}}{(L_j + S_j) \delta_j}, \quad (1)$$

$$\frac{\partial (C_{CO_2} u_g)}{\partial z} + \frac{\partial [r (C_{CO_2} v_g + \langle C'_{CO_2} v'_g \rangle)]}{r \partial r} = 6 \sum_{j=1}^{M_C} \frac{L_j S_j \beta_j C_{O_2}}{(L_j + S_j) \delta_j}, \quad (2)$$

$$\frac{\partial (C_{N_2} u_g)}{\partial z} + \frac{\partial [r (C_{N_2} v_g + \langle C'_{N_2} v'_g \rangle)]}{r \partial r} = 0, \quad (3)$$

where the subscript $j = 1 - M_C$ refers to the coke particles. The left-hand sides of (1)–(3) allow for the convective and pulsation transfer of the substance in the axial and radial directions, whereas the right-hand sides allow for the influence of the heterogeneous reaction $C + O_2 = CO_2$. Summing Eqs. (1)–(3) premultiplied by the corresponding molecular weights μ_{CO_2} , μ_{O_2} , and μ_{N_2} , we obtain the continuity equation for the gas mixture

$$\frac{\partial (\rho_g u_g)}{\partial z} + \frac{\partial [r (\rho_g v_g + \langle \rho'_g v'_g \rangle)]}{r \partial r} = 6 \sum_{j=1}^{M_C} \frac{(\mu_{CO_2} - \mu_{O_2}) L_j S_j \beta_j C_{O_2}}{(L_j + S_j) \delta_j}. \quad (4)$$

2. For the reacting coke particles, we write two continuity equations (it is taken into account that the number concentration of the particles n_j is unaffected by combustion, i.e., remains constant)

$$\frac{\partial (\beta_j \mu_{pj})}{\partial z} + \frac{\partial [r (\beta_j v_{pj} + \langle \beta'_j v'_{pj} \rangle)]}{r \partial r} = -\frac{6 \mu_C L_j S_j \beta_j C_{O_2}}{(L_j + S_j) \delta_j \rho_C}, \quad (5)$$

$$\frac{\partial (n_j \mu_{pj})}{\partial z} + \frac{\partial [r (n_j v_{pj} + \langle n'_j v'_{pj} \rangle)]}{r \partial r} = 0. \quad (6)$$

The size of the coke particles $\delta_j = \sqrt[3]{\frac{6\beta_j}{\pi n_j}}$ at each point of the flow is easily determined from the known values of β_j and n_j .

3. The mass equation of the ash particles is

$$\frac{\partial (\beta_l \mu_{pl})}{\partial z} + \frac{\partial [r (\beta_l v_{pl} + \langle \beta'_l v'_{pl} \rangle)]}{r \partial r} = 0, \quad (7)$$

where the subscript $l = 1 - M_{ash}$ refers to the ash particles. Unlike expression (5), the right-hand side of Eq. (7) is equal to zero, since the ash particles are not involved in combustion.

4. The equations of momentum transfer of the phases are

$$\rho_g u_g \frac{\partial u_g}{\partial z} + (\rho_g v_g + \langle \rho'_g v'_g \rangle) \frac{\partial u_g}{\partial r} = \frac{\partial}{r \partial r} \left[r \rho_g \left(\eta_g \frac{\partial u_g}{\partial r} - \langle u'_g v'_g \rangle \right) \right] - \frac{\partial P}{\partial z} - \sum_{i=1}^{M_C + M_{ash}} F_{aiz} + 6 \sum_{j=1}^{M_C} \frac{(\mu_{CO_2} - \mu_{O_2}) L_j S_j \beta_j C_{O_2}}{(L_j + S_j) \delta_j} (u_{pj} - u_g), \quad (8)$$

$$\rho_{pi} \left[\beta_i u_{pi} \frac{\partial u_{pi}}{\partial z} + (\beta_i v_{pi} + \langle \beta'_i v'_{pi} \rangle) \frac{\partial u_{pi}}{\partial r} \right] = - \frac{\rho_{pi}}{r} \frac{\partial (\beta_i r \langle u'_{pi} v'_{pi} \rangle)}{\partial r} + F_{aiz} + F_{coliz} - \rho_{pi} \beta_i g, \quad (9)$$

$$\rho_{pi} \left[\beta_i u_{pi} \frac{\partial v_{pi}}{\partial z} + (\beta_i v_{pi} + \langle \beta'_i v'_{pi} \rangle) \frac{\partial v_{pi}}{\partial r} \right] = - \frac{\rho_{pi}}{r} \frac{\partial [r (v_{pi} \langle \beta'_i v'_{pi} \rangle + \beta_i \langle v_{pi}^2 \rangle)]}{\partial r} + F_{air} + F_{colir} + \frac{\rho_{pi} \beta_i \langle w_{pi}^2 \rangle}{r}, \quad (10)$$

where the subscript i is equal to j and l . On the right-hand side of the equation of motion of the gas (8) are the viscous and Reynolds stresses, the pressure gradient, the inverse influence of particles on the gas, and the reaction force occurring on passage of the burnt carbon into the gaseous phase. Turbulent stresses, gravity, the interphase- and interparticle-interaction forces F_{coli} [3], and the centrifugal force due to the transverse pulsations of the particle velocity are allowed for in (9) and (10).

5. The equation of transfer of the turbulent gas energy is

$$\rho_g u_g \frac{\partial k_g}{\partial z} + (\rho_g v_g + \langle \rho'_g v'_g \rangle) \frac{\partial k_g}{\partial r} = \frac{\partial}{r \partial r} \left[r \rho_g \left(\frac{\eta_{t,g}}{\sigma_k} + \eta_g \right) \frac{\partial k_g}{\partial r} \right] + \rho_g \eta_{t,g} \left(\frac{\partial u_g}{\partial r} \right)^2 - \rho_g (\epsilon_g + \sum_{i=1}^{M_C + M_{ash}} \epsilon_{pi}) + \sum_{i=1}^{M_C + M_{ash}} G_{gi} - 6 \sum_{j=1}^{M_C} \frac{(\mu_{CO_2} - \mu_{O_2}) L_j S_j \beta_j C_{O_2}}{(L_j + S_j) \delta_j} (2k_g - \langle u'_{pj} u'_g \rangle - \langle v'_{pj} v'_g \rangle - \langle w'_{pj} w'_g \rangle), \quad (11)$$

where the double correlations $\langle u'_{pj} u'_g \rangle$, $\langle v'_{pj} v'_g \rangle$, and $\langle w'_{pj} w'_g \rangle$ are determined according to [5]. On the right-hand side of (11), the first term describes the molecular and turbulent transfer of pulsation energy, the second term describes its generation due to the energy of the averaged motion, the third term describes its dissipation due to the viscosity of the gaseous phase and the particles present in it, the fourth term describes the generation of turbulent energy in the wakes of the particles, and the last term describes the consumption of the turbulent gas energy by the new substance.

6. The energy equations of the phases are

$$c_g \rho_g u_g \frac{\partial t_g}{\partial z} + c_g (\rho_g v_g + \langle \rho'_g v'_g \rangle) \frac{\partial t_g}{\partial r} = \frac{\partial}{r \partial r} \left[r c_g \rho_g \left(\frac{\eta_g}{Pr_g} \frac{\partial t_g}{\partial r} - \langle t'_g v'_g \rangle \right) \right] + 10^{-3} u_g \frac{\partial P}{\partial z} + 10^{-3} \sum_{i=1}^{M_C + M_{ash}} F_{aiz} (u_g - u_{pi}) + \sum_{i=1}^{M_C + M_{ash}} \alpha_{\Sigma i} (t_{pi} - t_g) \frac{6 \beta_i}{\delta_i} + 6 \sum_{j=1}^{M_C} \frac{(\mu_{CO_2} - \mu_{O_2}) L_j S_j \beta_j C_{O_2}}{(L_j + S_j) \delta_j} \times \left[c_{pj} t_{pj} - c_g t_g + \frac{0.5 (u_g - u_{pj})^2}{10^3} \right] + 10^{-3} \rho_g \eta_{t,g} \left(\frac{\partial u_g}{\partial r} \right)^2, \quad (12)$$

$$c_{pi}\beta_i\mu_{pi}\frac{\partial t_{pi}}{\partial z} + c_{pi}(\beta_i\nu_{pi} + \langle\beta_i'\nu_{pi}'\rangle)\frac{\partial t_{pi}}{\partial r} = -\frac{\partial(r\beta_i c_{pi}\langle t_{pi}'\nu_{pi}'\rangle)}{rdr} - \alpha_{\Sigma_i}(t_{pi} - t_g)\frac{6\beta_i}{\delta_i\rho_{pi}} + \frac{6\omega_i L_i S_i \beta_i C_{O_2} Q_i}{(L_i + S_i)\delta_i\rho_{pi}}, \quad (13)$$

where $\omega_j = 1$ and $\omega_l = 0$. The molecular and turbulent transfer of the gas flow, the work of Reynolds stresses and pressure and interphase-interaction forces, the radiant and convective heat exchange between the gas and the particles, and the excess of the enthalpy and the deficiency of the kinetic energy of the part of the substance of coke particles that passes into the gas due to the heterogeneous reaction are allowed for in (12). In (13) are terms allowing for the pulsation heat transfer in the solid phase, heat transfer between the carrying medium and the dispersed phase, and heat release due to the heterogeneous chemical reaction. Integration of (4) over the reactor cross section yields

$$\frac{dB_g}{dz} = 12\pi \int_0^R \sum_{j=1}^{M_C} \frac{(\mu_{CO_2} - \mu_{O_2}) L_j S_j \beta_j C_{O_2}}{(L_j + S_j) \delta_j} r dr. \quad (14)$$

The correlations of second order $\langle\beta_i'\nu_{pi}'\rangle$, $\langle\rho_g'\nu_g'\rangle$, $\langle u_{pi}'\nu_{pi}'\rangle$, $\langle C_\chi'\nu_g'\rangle$, $\langle t_g'\nu_g'\rangle$, $\langle n_j'\nu_{pj}'\rangle$, and $\langle u_g'\nu_g'\rangle$ appearing in Eqs. (1)–(13) are computed on the basis of gradient representations

$$\begin{aligned} \langle\beta_i'\nu_{pi}'\rangle &= -J_{pi} \frac{\partial\beta_i}{\partial r}, \quad \langle\rho_g'\nu_g'\rangle = -J_g \frac{\partial\rho_g}{\partial r}, \quad \langle u_{pi}'\nu_{pi}'\rangle = -\eta_{t,pi} \frac{\partial u_{pi}}{\partial r}, \quad \langle C_\chi'\nu_g'\rangle = -J_g \frac{\partial C_\chi}{\partial r}, \\ \langle t_g'\nu_g'\rangle &= -\frac{\eta_{t,g}}{Pr_{t,g}} \frac{\partial t_g}{\partial r}, \quad \langle u_g'\nu_g'\rangle = -\eta_{t,g} \frac{\partial u_g}{\partial r}, \quad \langle n_j'\nu_{pj}'\rangle = -J_{pj} \frac{\partial n_j}{\partial r}, \end{aligned}$$

and the gas density ρ_g is calculated from the formula

$$\rho_g = \frac{10^{-3}P}{(t_g + 273)H \sum_{\chi=1}^3 \frac{Z_\chi}{\mu_\chi}},$$

where the subscripts $\chi = 1-3$ refer to O_2 , CO_2 , and N_2 . To close the system of equations (1)–(14) we must determine the unknown second moments $\langle v_{pi}^2 \rangle$, $\langle w_{pi}'w_{pi}' \rangle$, and $\langle t_{pi}'\nu_{pi}' \rangle$ appearing in Eqs. (10) and (13), which in turn are dependent on the Reynolds stresses $\langle w_{pi}'\nu_{pi}' \rangle$, $\langle u_{pi}^2 \rangle$, and $\langle t_{pi}'w_{pi}' \rangle$. To compute the above variables we use the developed computational procedure based on construction of the equations of transfer of the correlations sought [6, 7]. With this procedure, in the approximation of a narrow channel, we obtain a closed system of equations of momentum and heat transfer in the dispersed phase at the level of equations for the second moments of pulsations of particle velocity and temperature.

7. The equation of transfer of the normal Reynolds stress $\langle v_{pi}^2 \rangle$ is

$$\begin{aligned} \beta_i\mu_{pi} \frac{\partial \langle v_{pi}^2 \rangle}{\partial z} + (\beta_i\nu_{pi} + \langle\beta_i'\nu_{pi}'\rangle) \frac{\partial \langle v_{pi}^2 \rangle}{\partial r} &= \frac{\partial}{\partial r} \left(r\tau_i\beta_i \langle v_{pi}^2 \rangle \frac{\partial \langle v_{pi}^2 \rangle}{\partial r} \right) \\ &- \frac{2\partial(\tau_i\beta_i \langle w_{pi}'\nu_{pi}' \rangle^2)}{r\partial r} - 2\beta_i \langle v_{pi}'\nu_{pi}' \rangle \frac{\partial \nu_{pi}}{\partial r} - \frac{2\tau_i\beta_i \langle v_{pi}'\nu_{pi}' \rangle}{3r} \frac{\partial \langle w_{pi}^2 \rangle}{\partial r} \\ &- \frac{4\beta_i\tau_i \langle w_{pi}'\nu_{pi}' \rangle}{3r} \frac{\partial \langle w_{pi}'\nu_{pi}' \rangle}{\partial r} + \frac{4\beta_i\tau_i \langle w_{pi}^2 \rangle^2}{3r^2} - \frac{4\tau_i\beta_i \langle v_{pi}^2 \rangle \langle w_{pi}^2 \rangle}{3r^2} - \frac{4\beta_i\tau_i \langle w_{pi}'\nu_{pi}' \rangle^2}{3r^2} \end{aligned}$$

$$\begin{aligned}
& + \frac{2\beta_i (\langle v'_{pi} v'_g \rangle - \langle v_{pi}^2 \rangle)}{\tau_i} + 2 \left\{ \frac{\left[\frac{1-K_n}{2} - \frac{1-K_\tau}{7} \right]^2 \delta_m^2 \beta_i}{6912\beta_m^2} \left(\frac{\partial u_{pi}}{\partial r} \right)^2 N_{\Sigma i, i} \right. \\
& + \sum_{\substack{i=1 \\ y \neq i}}^{M_C + M_{ash}} \frac{\left(1 - K_n - \frac{2(1-K_\tau)}{7} \right)^2 |u_{py} - u_{pi}|^2 \beta_i m_y^2 N_{\Sigma y, i}}{24(m_y + m_i)^2} \\
& \left. - \sum_{i=1}^{M_C + M_{ash}} U_1 \frac{\left[1 - \left(\frac{1-K_n}{2} - \frac{1-K_\tau}{7} \right)^2 \right] \langle |\mathbf{V}'_{py, i}| \rangle^2 \beta_i m_y^2 N_{\Sigma y, i}}{3(m_y + m_i)^2} \right\}, \quad K_n < 0, \quad (15)
\end{aligned}$$

where $y = 1 - M_C + M_{ash}$, $\langle |\mathbf{V}'_{py, i}| \rangle^2$ is the mean relative velocity squared of y and i particles in random motion [8], and $N_{\Sigma i, i}$ and $N_{\Sigma y, i}$ are the total frequencies of collisions of mono- and polydisperse particles, which involve collisions due to the difference of the averaged axial velocities of the particles [3, 8] and their random motion [8].

8. The equation of transfer of the second moment $\langle w_{pi}^2 \rangle$ is

$$\begin{aligned}
& \beta_i u_{pi} \frac{\partial \langle w_{pi}^2 \rangle}{\partial z} + (\beta_i v_{pi} + \langle \beta'_i v'_{pi} \rangle) \frac{\partial \langle w_{pi}^2 \rangle}{\partial r} = \frac{\partial}{\partial r} \left(r \tau_i \beta_i \langle v_{pi}^2 \rangle \frac{\partial \langle w_{pi}^2 \rangle}{\partial r} \right) \\
& + \frac{2\partial}{\partial r} \left(r \tau_i \beta_i \langle w'_{pi} v'_{pi} \rangle \frac{\partial \langle w'_{pi} v'_{pi} \rangle}{\partial r} \right) - \frac{2\partial (\tau_i \beta_i \langle w_{pi}^2 \rangle^2)}{3r\partial r} + \frac{2\partial (\tau_i \beta_i \langle v_{pi}^2 \rangle \langle w_{pi}^2 \rangle)}{3r\partial r} \\
& + \frac{2\partial (\tau_i \beta_i \langle w'_{pi} v'_{pi} \rangle^2)}{3r\partial r} - \frac{2\beta_i v_{pi} \langle w_{pi}^2 \rangle}{r} + \frac{2\tau_i \beta_i \langle v_{pi}^2 \rangle \partial \langle w_{pi}^2 \rangle}{3r\partial r} \\
& + \frac{4\tau_i \beta_i \langle w'_{pi} v'_{pi} \rangle \partial \langle w'_{pi} v'_{pi} \rangle}{3r\partial r} - \frac{4\tau_i \beta_i \langle w_{pi}^2 \rangle^2}{3r^2} + \frac{4\tau_i \beta_i \langle v_{pi}^2 \rangle \langle w_{pi}^2 \rangle}{3r^2} + \frac{4\tau_i \beta_i \langle w'_{pi} v'_{pi} \rangle^2}{3r^2} \\
& + \frac{2\beta_i}{\tau_i} (\langle w'_{pi} w'_g \rangle - \langle w_{pi}^2 \rangle) + 2 \left\{ \frac{\left[\frac{1-K_n}{2} - \frac{1-K_\tau}{7} \right]^2 \delta_m^2 \beta_i}{6912\beta_m^2} \left(\frac{\partial u_{pi}}{\partial r} \right)^2 N_{\Sigma i, i} \right. \\
& + \sum_{\substack{i=1 \\ y \neq i}}^{M_C + M_{ash}} \frac{\left(1 - K_n - \frac{2(1-K_\tau)}{7} \right)^2 |u_{py} - u_{pi}|^2 \beta_i m_y^2 N_{\Sigma y, i}}{24(m_y + m_i)^2}
\end{aligned}$$

$$- \sum_{i=1}^{M_C+M_{\text{ash}}} U_2 \frac{\left[1 - \left(\frac{1-K_n}{2} - \frac{1-K_\tau}{7} \right)^2 \right] \langle |\mathbf{V}'_{py,i}| \rangle^2 \beta_i m_y^2 N_{\Sigma y,i}}{3(m_y + m_i)^2} \Bigg\}. \quad (16)$$

9. The equation of transfer of the tangential Reynolds stress $\langle w'_{pi} v'_{pi} \rangle$ is

$$\begin{aligned} \beta_i \mu_{pi} \frac{\partial \langle w'_{pi} v'_{pi} \rangle}{\partial z} + (\beta_i v_{pi} + \langle \beta'_i v'_{pi} \rangle) \frac{\partial \langle w'_{pi} v'_{pi} \rangle}{\partial r} &= \frac{2\partial}{3r\partial r} \left(\beta_i r \tau_i \langle v_{pi}^{\prime 2} \rangle \frac{\partial \langle w'_{pi} v'_{pi} \rangle}{\partial r} \right) \\ - \beta_i \langle w'_{pi} v'_{pi} \rangle \frac{\partial v_{pi}}{\partial r} + \frac{2\partial (\beta_i \tau_i \langle v_{pi}^{\prime 2} \rangle \langle w'_{pi} v'_{pi} \rangle)}{3r\partial r} + \frac{\partial}{3r\partial r} \left(r \beta_i \tau_i \langle w'_{pi} v'_{pi} \rangle \frac{\partial \langle v_{pi}^{\prime 2} \rangle}{\partial r} \right) \\ - \frac{4\partial (\beta_i \tau_i \langle w'_{pi} v'_{pi} \rangle \langle w_{pi}^{\prime 2} \rangle)}{3r\partial r} - \frac{\beta_i \tau_i \langle w'_{pi} v'_{pi} \rangle}{r} \frac{\partial \langle w_{pi}^{\prime 2} \rangle}{\partial r} - \frac{10\beta_i \tau_i \langle w'_{pi} v'_{pi} \rangle \langle w_{pi}^{\prime 2} \rangle}{3r^2} \\ - \frac{\beta_i v_{pi} \langle w'_{pi} v'_{pi} \rangle}{r} + \frac{2\tau_i \beta_i \langle v_{pi}^{\prime 2} \rangle}{3r} \frac{\partial \langle w'_{pi} v'_{pi} \rangle}{\partial r} + \frac{2\beta_i \tau_i \langle v_{pi}^{\prime 2} \rangle \langle w'_{pi} v'_{pi} \rangle}{3r^2} \\ + \frac{\beta_i \tau_i \langle w'_{pi} v'_{pi} \rangle}{3r} \frac{\partial \langle v_{pi}^{\prime 2} \rangle}{\partial r} + \frac{\beta_i (\langle v'_g w'_{pi} \rangle + \langle v'_{pi} w'_g \rangle - 2 \langle w'_{pi} v'_{pi} \rangle)}{\tau_i}. \end{aligned} \quad (17)$$

10. The equation for the axial component of the pulsation particle energy $\langle u_{pi}^{\prime 2} \rangle$ is

$$\begin{aligned} \beta_i \mu_{pi} \frac{\partial \langle u_{pi}^{\prime 2} \rangle}{\partial z} + (\beta_i v_{pi} + \langle \beta'_i v'_{pi} \rangle) \frac{\partial \langle u_{pi}^{\prime 2} \rangle}{\partial r} &= \frac{\partial}{3r\partial r} \left(\beta_i r \tau_i \langle v_{pi}^{\prime 2} \rangle \frac{\partial \langle u_{pi}^{\prime 2} \rangle}{\partial r} \right) \\ + 2\beta_i \tau_i \langle v_{pi}^{\prime 2} \rangle \left(\frac{\partial u_{pi}}{\partial r} \right) + \frac{2\beta_i}{\tau_i} (\langle u'_{pi} u'_g \rangle - \langle u_{pi}^{\prime 2} \rangle) + 2 \left\{ \frac{\left[\frac{1-K_n}{2} - \frac{1-K_\tau}{7} \right]^2 \delta_m^2 \beta_i}{6912\beta_m^2} \left(\frac{\partial u_{pi}}{\partial r} \right)^2 N_{\Sigma i,i} \right. \\ + \sum_{\substack{i=1 \\ y \neq i}}^{M_C+M_{\text{ash}}} \frac{\left(1 - K_n - \frac{2(1-K_\tau)}{7} \right)^2 |u_{py} - u_{pi}|^2 \beta_i m_y^2 N_{\Sigma y,i}}{24(m_y + m_i)^2} \\ \left. - \sum_{i=1}^{M_C+M_{\text{ash}}} U_3 \frac{\left[1 - \left(\frac{1-K_n}{2} - \frac{1-K_\tau}{7} \right)^2 \right] \langle |\mathbf{V}'_{py,i}| \rangle^2 \beta_i m_y^2 N_{\Sigma y,i}}{3(m_y + m_i)^2} \right\}. \end{aligned} \quad (18)$$

In the present work, we consider two approaches to determination of the correlation of second order $\langle t'_{pi} v'_{pi} \rangle$, which are based on the use of the gradient representations $\langle t'_{pi} v'_{pi} \rangle = \frac{\eta_{t,pi}}{Pr_{t,pi}} \frac{\partial t_{pi}}{\partial r}$ and the equations of transfer of second moments.

11. The equation of transfer of the correlation $\langle t'_{pi} v'_{pi} \rangle$ is

$$\begin{aligned} \beta_i \mu_{pi} \frac{\partial \langle t'_{pi} v'_{pi} \rangle}{\partial z} + (\beta_i v_{pi} + \langle \beta'_i v'_{pi} \rangle) \frac{\partial \langle t'_{pi} v'_{pi} \rangle}{\partial r} &= \frac{\partial}{r \partial r} \left(\frac{\beta_i r \langle v_{pi}^2 \rangle}{\Psi_{1i}} \frac{\partial \langle t'_{pi} v'_{pi} \rangle}{\partial r} \right) \\ + \frac{\partial}{2r \partial r} \left(\frac{\beta_i r \langle t'_{pi} v'_{pi} \rangle}{\Psi_{1i}} \frac{\partial \langle v_{pi}^2 \rangle}{\partial r} \right) - \frac{2 \partial}{r \partial r} \left(\frac{\beta_i \langle w'_{pi} v'_{pi} \rangle \langle t'_{pi} w'_{pi} \rangle}{\Psi_{1i}} \right) - \frac{\beta_i \langle v_{pi}^2 \rangle}{\partial r} \frac{\partial t_{pi}}{\partial r} \\ - \frac{\beta_i \langle t'_{pi} v'_{pi} \rangle}{\partial r} \frac{\partial v_{pi}}{\partial r} - \frac{\beta_i \langle w'_{pi} v'_{pi} \rangle}{\Psi_{1i} r \partial r} \frac{\partial \langle t'_{pi} w'_{pi} \rangle}{\partial r} - \frac{\beta_i \langle t'_{pi} v'_{pi} \rangle}{2 \Psi_{1i} r \partial r} \frac{\partial \langle w_{pi}^2 \rangle}{\partial r} \\ - \frac{\beta_i \langle w'_{pi} v'_{pi} \rangle \langle t'_{pi} w'_{pi} \rangle}{\Psi_{1i} r^2} - \frac{\beta_i \langle t'_{pi} v'_{pi} \rangle \langle w_{pi}^2 \rangle}{\Psi_{1i} r^2} + \frac{\beta_i (\langle t'_{pi} v'_{pi} \rangle - \langle t'_{pi} v'_{pi} \rangle)}{\tau_i} \\ + \frac{6 \beta_i \alpha_{\Sigma i} (\langle t'_{g} v'_{pi} \rangle - \langle t'_{pi} v'_{pi} \rangle)}{\rho_{pi} c_{pi} \delta_i}, \quad \Psi_{1i} = \frac{3 \alpha_{\Sigma i}}{\rho_{pi} c_{pi} \delta_i} + \frac{1}{\tau_i}. \end{aligned} \quad (19)$$

12. The equation of transfer of the correlation $\langle t'_{pi} w'_{pi} \rangle$ is

$$\begin{aligned} \beta_i \mu_{pi} \frac{\partial \langle t'_{pi} w'_{pi} \rangle}{\partial z} + (\beta_i v_{pi} + \langle \beta'_i v'_{pi} \rangle) \frac{\partial \langle t'_{pi} w'_{pi} \rangle}{\partial r} &= \frac{\partial}{r \partial r} \left(\frac{\beta_i r \langle v_{pi}^2 \rangle}{\Psi_{2i}} \frac{\partial \langle t'_{pi} w'_{pi} \rangle}{\partial r} \right) \\ + \frac{\partial}{r \partial r} \left(\frac{\beta_i r \langle t'_{pi} v'_{pi} \rangle}{\Psi_{2i}} \frac{\partial \langle w'_{pi} v'_{pi} \rangle}{\partial r} \right) + \frac{\partial}{r \partial r} \left(\frac{\beta_i \langle t'_{pi} v'_{pi} \rangle \langle w'_{pi} v'_{pi} \rangle}{\Psi_{2i}} \right) \\ + \frac{\partial}{r \partial r} \left(\frac{\beta_i r \langle w'_{pi} v'_{pi} \rangle}{\Psi_{2i}} \frac{\partial \langle t'_{pi} v'_{pi} \rangle}{\partial r} \right) - \frac{2 \partial}{r \partial r} \left(\frac{\beta_i \langle t'_{pi} w'_{pi} \rangle \langle w_{pi}^2 \rangle}{\Psi_{2i}} \right) \\ + \frac{\partial}{r \partial r} \left(\frac{\beta_i \langle v_{pi}^2 \rangle \langle t'_{pi} w'_{pi} \rangle}{\Psi_{2i}} \right) - \frac{\beta_i \langle w'_{pi} v'_{pi} \rangle}{\partial r} \frac{\partial t_{pi}}{\partial r} - \frac{\beta_i v_{pi} \langle t'_{pi} w'_{pi} \rangle}{r} + \frac{\beta_i \langle v_{pi}^2 \rangle}{\Psi_{2i}} \frac{\partial \langle t'_{pi} w'_{pi} \rangle}{r \partial r} \\ + \frac{\beta_i \langle t'_{pi} v'_{pi} \rangle}{\Psi_{2i}} \frac{\partial \langle w'_{pi} v'_{pi} \rangle}{r \partial r} + \frac{\beta_i \langle t'_{pi} v'_{pi} \rangle \langle w'_{pi} v'_{pi} \rangle}{\Psi_{2i} r^2} + \frac{\beta_i \langle w'_{pi} v'_{pi} \rangle}{\Psi_{2i}} \frac{\partial \langle t'_{pi} v'_{pi} \rangle}{r \partial r} \\ - \frac{2 \beta_i \langle w_{pi}^2 \rangle \langle t'_{pi} w'_{pi} \rangle}{\Psi_{2i} r^2} + \frac{\beta_i \langle v_{pi}^2 \rangle \langle t'_{pi} w'_{pi} \rangle}{\Psi_{2i} r^2} + \frac{\beta_i (\langle t'_{pi} w'_{pi} \rangle - \langle t'_{pi} w'_{pi} \rangle)}{\tau_i} \end{aligned}$$

$$+ \frac{6\beta_i \alpha_{\Sigma i} (\langle t'_g w'_{pi} \rangle - \langle t'_{pi} w'_{pi} \rangle)}{\rho_{pi} c_{pi} \delta_i}, \quad \Psi_{2i} = \frac{6\alpha_{\Sigma i}}{\rho_{pi} c_{pi} \delta_i} + \frac{2}{\tau_i}. \quad (20)$$

The mixed correlation moments $\langle v'_g w'_{pi} \rangle$, $\langle v'_{pi} w'_g \rangle$, $\langle t'_g v'_{pi} \rangle$, $\langle t'_{pi} v'_g \rangle$, $\langle t'_{pi} w'_g \rangle$, and $\langle t'_g w'_{pi} \rangle$ present in Eqs. (17), (19), and (20) are determined in terms of the correlations of the carrying flow in a locally homogeneous approximation in accordance with the recommendations of [5]. In Eqs. (15), (16), and (18) are additional terms of nonturbulent origin (the last three terms of the equations) that describe the generation and dissipation of turbulent energy, caused by interparticle collisions due to the averaged and pulsation particle motion. As has been noted in [3, 8], these terms cannot be computed by the traditional methods of turbulence theory, since pulsations related to interparticle interactions are mainly dependent on the random position of a unit vector directed along the line of impact. Therefore, a specially developed computational procedure based on an analysis of the dynamics of the process of collisions was used to determine these terms [3, 8].

Boundary Conditions and Computational Algorithm. Boundary conditions for Eqs. (1)–(13) and (15)–(20) on the flow axis are specified for reasons of symmetry ($r = 0$)

$$\begin{aligned} \frac{\partial C_\chi}{\partial r} = \frac{\partial u_g}{\partial r} = \frac{\partial k_g}{\partial r} = \frac{\partial \beta_i}{\partial r} = \frac{\partial n_j}{\partial r} = v_g = v_{pi} = 0, \\ \frac{\partial u_{pi}}{\partial r} = \frac{\partial \langle v'_{pi} v'_{pi} \rangle}{\partial r} = \frac{\partial \langle w'_{pi} w'_{pi} \rangle}{\partial r} = \frac{\partial \langle u'_{pi} u'_{pi} \rangle}{\partial r} = \frac{\partial \langle w'_{pi} v'_{pi} \rangle}{\partial r} = 0, \\ \frac{\partial t_g}{\partial r} = \frac{\partial t_{pi}}{\partial r} = \frac{\partial \langle t'_{pi} v'_{pi} \rangle}{\partial r} = \frac{\partial \langle t'_{pi} w'_{pi} \rangle}{\partial r} = 0, \end{aligned} \quad (21)$$

on the channel wall ($r = R$), they are specified by the relations

$$\begin{aligned} v_{pi} = u_g = k_g = \frac{\partial \beta_i}{\partial r} = \frac{\partial n_j}{\partial r} = \frac{\partial C_\chi}{\partial r} = 0, \quad u_{pi} = \frac{\delta_i}{24\sqrt{2} \beta_i (1 - K_\tau)} \left(\frac{\partial u_{pi}}{\partial r} \right) (7K_n - 2K_\tau - 5), \\ \langle v'_{pi} v'_{pi} \rangle = \frac{K_n \delta_i}{12\sqrt{2} \beta_i (1 + K_n)} \left(\frac{\partial \langle v'_{pi} v'_{pi} \rangle}{\partial r} \right), \quad \langle w'_{pi} w'_{pi} \rangle = \frac{\left[K_n - \frac{(5 + 2K_\tau)^2}{49} \right] \delta_i}{12\sqrt{2} \beta_i \left[1 - \frac{(5 + 2K_\tau)^2}{49} \right]} \left(\frac{\partial \langle w'_{pi} w'_{pi} \rangle}{\partial r} \right), \\ \frac{\partial t_{pi}}{\partial r} = \frac{\partial \langle t'_{pi} v'_{pi} \rangle}{\partial r} = \frac{\partial \langle t'_{pi} w'_{pi} \rangle}{\partial r} = 0, \quad \langle w'_{pi} v'_{pi} \rangle = \frac{K_n (6 + K_\tau) \delta_i}{6\sqrt{2} \beta_i [7 + K_n (5 + 2K_\tau)]} \left(\frac{\partial \langle w'_{pi} v'_{pi} \rangle}{\partial r} \right), \\ \langle u'_{pi} u'_{pi} \rangle = \frac{\left[\frac{(5 + 2K_\tau)^2}{49} - K_n \right] \delta_i}{12\sqrt{2} \beta_i \left[\frac{(5 + 2K_\tau)^2}{49} - 1 \right]} \left(\frac{\partial \langle u'_{pi} u'_{pi} \rangle}{\partial r} \right), \quad t_g = t_w. \end{aligned} \quad (22)$$

Thus, we have obtained two closed systems of Eqs. (1)–(18) (first case) and (1)–(20) (second case) that differ in the manner in which Eq. (13) is closed. In the first case we use the Boussinesq hypothesis to determine $\langle t'_{pi} v'_{pi} \rangle$, whereas in the second case we use the equations of transfer of second moments (19) and (20). The complete system of Eqs. (1)–(20) with boundary conditions (21) and (22) contains equations of three types. The parabolic equations

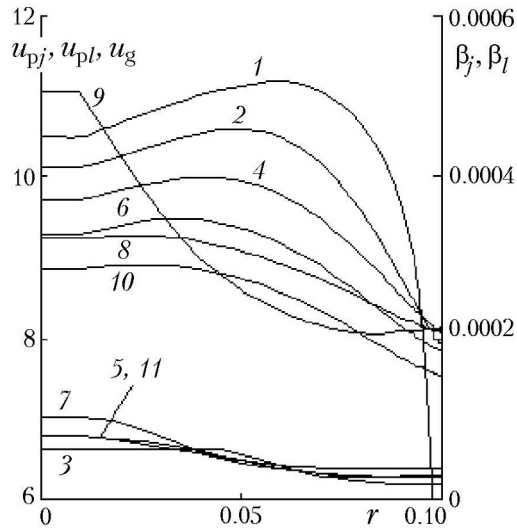


Fig. 1. Distribution of the averaged axial velocities of phases and the volume concentrations of particles over the reactor cross section at the mark $z = 6$ m for variant I: 1) u_g , 2) u_{C1} , 3) β_{C1} , 4) u_{C3} , 5) β_{C3} , 6) u_{C2} , 7) β_{C2} , 8) u_{ash} , 9) β_{ash} , 10) u_{C4} , and 11) β_{C4} .

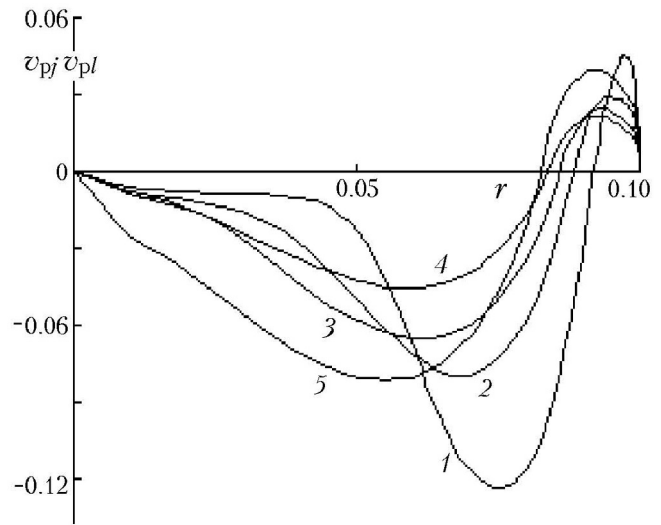


Fig. 2. Distribution of the averaged radial velocities of coke particles of diameter δ_{C0} : 1) $0.15 \cdot 10^{-3}$ m, 2) $0.25 \cdot 10^{-3}$ m, 3) $0.35 \cdot 10^{-3}$ m, and 4) $0.45 \cdot 10^{-3}$ m, and of ash particles 5) $\delta_{ash} = 0.3 \cdot 10^{-3}$ m over the reactor cross section at the mark $z = 6$ m for variant I.

(1)–(3), (5)–(9), (11)–(13) (first case), and (15)–(20) and the hyperbolic equations (10) and (13) (second case) were integrated by the method of direct and reverse marchings on a nonuniform grid bunching at the channel wall. To solve the parabolic equations we used the iteration method, whereas no iterations were required for the equations of first order. The continuity equation of the carrying medium (4) from which the radial gas velocity is determined was approximated by the implicit four-point scheme. On the basis of the described algorithms, we developed two programs using which the aerodynamics, heat and mass exchange, and combustion of a polydisperse ensemble of coke-ash particles of anthracite culm in an axisymmetric channel were numerically investigated.

Certain Calculation Results. Let us discuss results of calculations of four variants with the following initial data. Variant I: $u_{g,m0} = 10$ m/sec, $Z_{O_2,0} = 0.1$, $R = 0.1$ m, $\delta_{C01} = 0.15 \cdot 10^{-3}$ m, $\delta_{C02} = 0.35 \cdot 10^{-3}$ m, $\delta_{C03} = 0.25 \cdot 10^{-3}$ m, $\delta_{C04} = 0.45 \cdot 10^{-3}$ m, $\delta_{ash} = 0.3 \cdot 10^{-3}$ m, $\beta_{C01} = \beta_{C02} = \beta_{C03} = \beta_{C04} = 0.0001$, $\beta_{ash} = 0.0006$, and $B_{g0} = 362$ kg/h (first case); II: $u_{g,m0} = 10$ m/sec, $Z_{O_2,0} = 0.1$, $R = 0.9$ m, $\delta_{C01} = 0.2 \cdot 10^{-3}$ m, $\delta_{C02} = 0.3 \cdot 10^{-3}$ m, $\delta_{C03} = 0.4 \cdot 10^{-3}$ m, $\delta_{ash} = 0.15 \cdot 10^{-3}$ m, $\beta_{C01} = \beta_{C02} = \beta_{C03} = 0.0001$, $\beta_{ash} = 0.0008$, and $B_{g0} = 29,210$ kg/h (first case); III: the values of the quantities $u_{g,m0}$, $Z_{O_2,0}$, R , δ_i , β_i , and B_{g0} are the same as those in variant II, $\beta_{ash} = 0.00035$ (first case); IV: $u_{g,m0} = 16$ m/sec, $Z_{O_2,0} = 0.12$, $R = 0.1$ m, $\delta_{C01} = 0.15 \cdot 10^{-3}$ m, $\delta_{C02} = 0.25 \cdot 10^{-3}$ m, $\delta_{C03} = 0.35 \cdot 10^{-3}$ m, $\delta_{ash} = 0.15 \cdot 10^{-3}$ m, $\beta_{C01} = \beta_{C02} = \beta_{C03} = 0.0001$, $\beta_{ash} = 0.00075$, and $B_{g0} = 574$ kg/h (second case). In all variants, we have $\rho_C = 1300$ kg/m³, $\rho_{ash} = 1800$ kg/m³, $t_{pi0} = t_{g0} = 900^\circ\text{C}$, and $t_w = 800^\circ\text{C}$. The calculated material is illustrated in Figs. 1–9 where the profiles of the averaged and pulsation characteristics of the nonisothermal gas-dispersed flow are presented. Figure 1 shows the calculated values of the averaged longitudinal gas velocity (curve 1). It is noteworthy that the maximum of the $u_g(r)$ profile is in the peripheral region. The reason is as follows. In much of the reactor cross section (except for the wall zone) where the particle velocity v_{pi} is negative (Fig. 2), the radial motion of the dispersed phase is directed to the flow axis because of which the maximum of the function $\beta_i(r)$ is formed at the axis and the minimum is formed in the peripheral zone (Fig. 1, curves 3, 5, 7, 9, and 11). This trend of variation in the $\beta_i(r)$ plot leads to the fact that the axial component of the aerodynamic force in the axial zone becomes larger than that in the peripheral zone. Therefore, the gas velocity decreases at the axis and grows in the wall region.

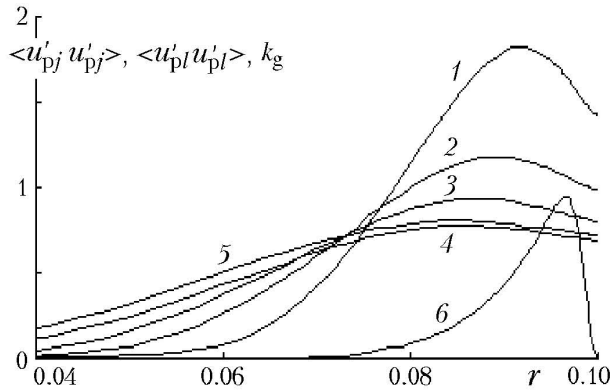


Fig. 3. Distribution of the axial component of the pulsation energy of coke particles of diameter δ_{C0} : 1) $0.15 \cdot 10^{-3}$ m, 2) $0.25 \cdot 10^{-3}$ m, 3) $0.35 \cdot 10^{-3}$ m, and 4) $0.45 \cdot 10^{-3}$ m, of the ash 5) $\delta_{ash} = 0.3 \cdot 10^{-3}$ m, and of the turbulent gas energy 6) k_g over the reactor cross section at the mark $z = 6$ for variant I.

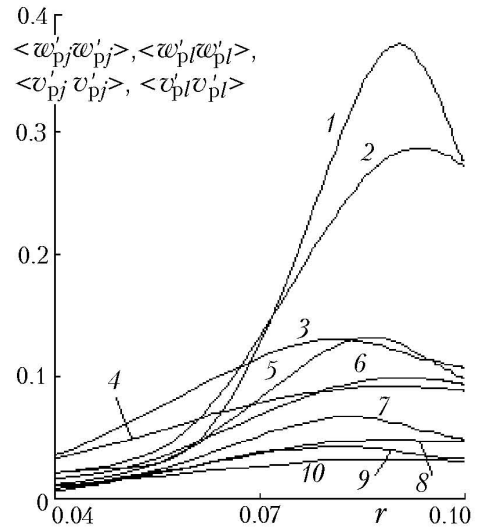


Fig. 4. Distribution of the second moments of pulsations of the translational velocity of particles over the reactor cross section at the mark $z = 6$ m for variant I: 1) $\langle w'_{C1} w'_{C1} \rangle$, 2) $\langle v'_{C1} v'_{C1} \rangle$, 3) $\langle w'_{ash} w'_{ash} \rangle$, 4) $\langle v'_{ash} v'_{ash} \rangle$, 5) $\langle w'_{C3} w'_{C3} \rangle$, 6) $\langle v'_{C3} v'_{C3} \rangle$, 7) $\langle w'_{C2} w'_{C2} \rangle$, 8) $\langle v'_{C2} v'_{C2} \rangle$, 9) $\langle w'_{C4} w'_{C4} \rangle$, and 10) $\langle v'_{C4} v'_{C4} \rangle$.

Figures 3 and 4 give the profiles of turbulent energy of the gas and components of the pulsation energy of particles. It is seen that the energy of random motion of the dispersed phase $k_{pi} = 0.5(\langle v_{pi}^2 \rangle + \langle w_{pi}^2 \rangle + \langle u_{pi}^2 \rangle)$ is much higher than the pulsation energy of the carrying medium k_g . This is due to the dissipation of the quantity k_g , caused by the presence of the particles in the gas and by the expenditure of the turbulent energy of the gas mixture on involving carbon dioxide in pulsatory motion (see (11)). The latter is formed by the heterogeneous reaction $C + O_2 = CO_2$. We should note another important feature of the process in question. In the peripheral zone, the components of the pulsation energy of small coke particles $\delta_{C01} = 0.15 \cdot 10^{-3}$ m are much higher than those of large particles $\delta_{C04} =$

$0.45 \cdot 10^{-3}$ m. For example., the ratio of the axial pulsation-energy components is $\left[\frac{\langle u'_{C1} u'_{C1} \rangle}{\langle u'_{C4} u'_{C4} \rangle} \right]_{r=0.091} = 2.4$ (Fig. 3,

curves 1 and 4), and that of the transverse components is $\left[\frac{\langle w'_{C1} w'_{C1} \rangle}{\langle w'_{C4} w'_{C4} \rangle} \right]_{r=0.091} = 10$ (Fig. 4, curves 1 and 9). The reason

is that the rate of generation of the pseudoturbulent energy of particles i in interaction of the $y-i$ fractions is proportional to m_y^2 (penultimate terms of Eqs. (15), (16), and (18)). From Figs. 3 and 4 it is clear that the quantities

$\langle w'_{C1} w'_{C1} \rangle$ and $\langle v'_{C1} v'_{C1} \rangle$ differ little (Fig. 4, curves 1 and 2), whereas the ratio $\left[\frac{\langle u'_{C1} u'_{C1} \rangle}{\langle w'_{C1} w'_{C1} \rangle} \right]_{r=0.091}$ is equal to 4.9,

which speaks of the anisotropy of the field of pulsation energy of the dispersed phase.

Figure 5 illustrates the thermal state of the two-phase flow with a polydisperse composition of coke particles. In the axial zone where the concentration of the coke is maximum (Fig. 1, curves 3, 5, 7, and 11), we have intense oxygen burning (Fig. 5, curve 7), because of which the heat released from the coke particles exceeds (convective +

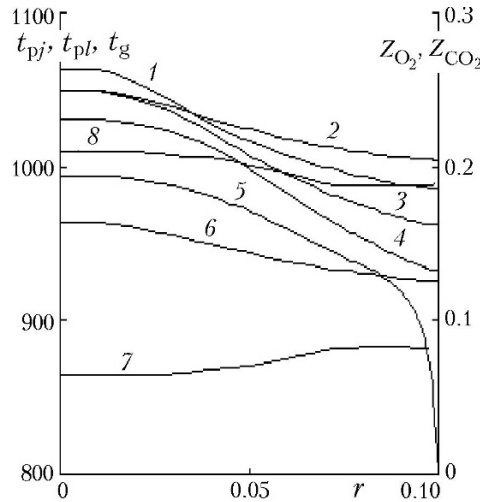


Fig. 5. Distribution of the averaged phase temperatures and the mass concentrations of O_2 and CO_2 in the gas mixture over the reactor cross section at the mark $z = 6$ m for variant I: 1) t_{C2} , 2) t_{C4} , 3) t_{C3} , 4) t_{C1} , 5) t_g , 6) t_{ash} , 7) Z_{O_2} , and 8) Z_{CO_2} .

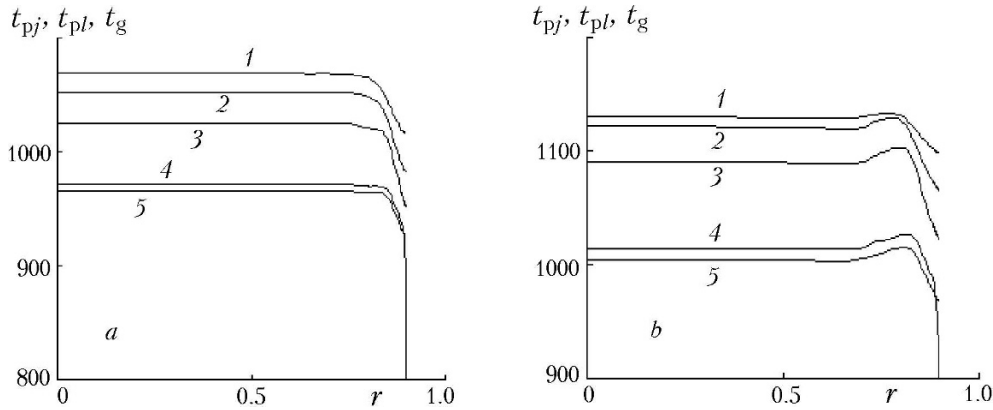


Fig. 6. Distribution of the averaged phase temperatures over the reactor cross section at the mark $z = 7$ m for variants II (a) and III (b): 1) t_{C3} , 2) t_{C2} , 3) t_{C1} , 4) t_g , and 5) t_{ash} .

radiant) the heat removed, which ensures their efficient burning, whose intensity increases toward the flow axis. Therefore, the coke temperature is higher than the gas and ash-particle temperature. Convective heat exchange becomes the determining factor of thermal state of carbon particles near the wall (due to the growth in the temperature head $t_j - t_g$), which leads to their cooling.

The reactor radius exerts a great influence on the distribution of the phase temperatures and the efficiency of coke burning. For low R values ($R = 0.1$ m), we have a significant variation in the phase temperature along the radial axis (Fig. 5, curves 1–6), whereas for high values ($R = 0.9$ m), the $t_g(r)$ and $t_i(r)$ plots are virtually constant in much of the reactor cross section (except for the wall zone) (Fig. 6). It is noteworthy that the maximum of the function $\beta_j(r)$ shifts from the axis to the wall region with increase in the channel radius (Figure 1, curves 3, 5, 7, and 11, and Fig. 7, curves 3–5, are compared). Here we observe an intense burning of the oxidizer (Fig. 7, curve 1), which contributes to the formation of the maximum of the $t_g(r)$ and $t_i(r)$ curves in this region (Fig. 6b). This regime of combustion of the polydisperse coke-ash mixture is hazardous, since for high Z_{O_2} and β_j values in the peripheral zone, the temperature of the ash particles near the wall can turn out to be higher than the temperature of the beginning of softening of the ash, which will lead to slagging of the reactor. One method of eliminating this hazard is to increase the ash concentration in the dispersed phase (Fig. 6a, curve 5).

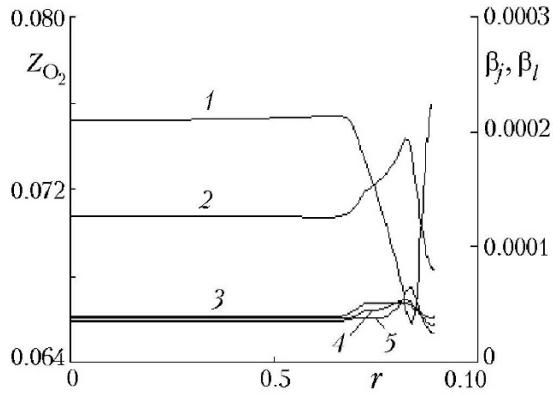


Fig. 7. Distribution of the mass concentration of O_2 in the gas mixture and the volume concentrations of particles over the reactor cross section at the mark $z = 7$ m for variant III: 1) Z_{O_2} , 2) β_{ash} , 3) β_{C3} , 4) β_{C2} , and 5) β_{C1} .

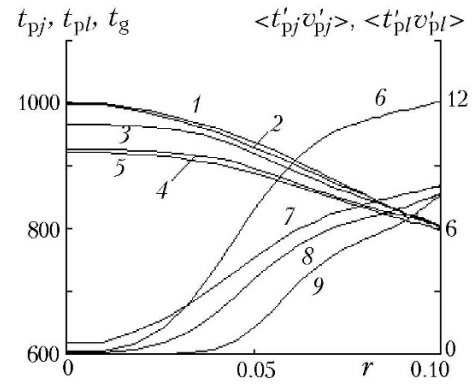


Fig. 8. Distribution of the averaged phase temperatures and the mixed correlation moments of pulsations of the particle temperature and radial velocity over the reactor cross section at the mark $z = 6$ m for variant IV: 1) t_{C3} , 2) t_{C2} , 3) t_{C1} , 4) t_g , 5) t_{ash} , 6) $\langle t'_{ash}v'_{ash} \rangle$, 7) $\langle t'_{C3}v'_{C3} \rangle$, 8) $\langle t'_{C2}v'_{C2} \rangle$, and 9) $\langle t'_{C1}v'_{C1} \rangle$.

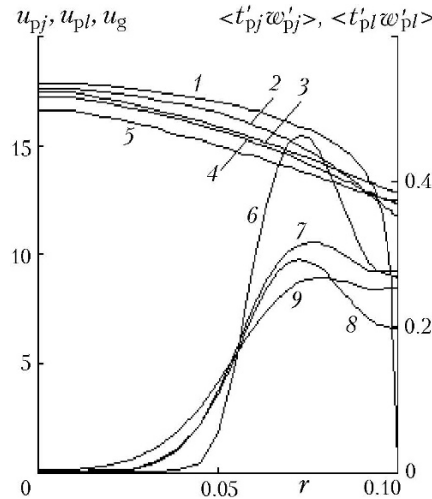


Fig. 9. Distribution of the averaged axial phase velocities and the second moments of pulsations of the particle temperature and transverse velocity over the reactor cross section at the mark $z = 6$ m for variant IV: 1) u_g , 2) u_{C1} , 3) u_{ash} , 4) u_{C2} , 5) u_{C3} , 6) $\langle t'_{C1}w'_{C1} \rangle$, 7) $\langle t'_{C2}w'_{C2} \rangle$, 8) $\langle t'_{ash}w'_{ash} \rangle$, and 9) $\langle t'_{C3}w'_{C3} \rangle$.

Figure 8 gives the calculated values of the phase temperatures and the correlations of second order of pulsations of the radial velocity and temperature of the dispersed phase for variant IV (second case). It is seen that the temperature of the coke particles decreases with their size at all points of the reactor cross section. Near the flow axis, the temperature of large and medium coke particles is virtually equal (curves 1 and 2). This is due, on the one hand, to the intense burning, and on the other hand, to the influence of interparticle collisions on the residence time of particles of different fractions.

Figure 9 gives the profiles of longitudinal velocities of the phases and second moments of fluctuations of the transverse velocity and temperature of particles. In the flow core, the particles lag behind the gas, and the larger the particles, the higher their free-fall velocity; in the wall zone, the particles lead the gas: here, the interphase-interaction force is negative and the suspension of the particles is related to their random motion.

It is noteworthy that the $\langle t'_{pi}w'_{pi} \rangle(r)$ plot has its maximum at the point $r = 0.073$ m (Fig. 9, curve 6). The balance of the terms of Eq. (20) shows that the dominant role in the formation of the $\langle t'_{pi}w'_{pi} \rangle(r)$ profile is played by the seventh $\frac{\beta_i \langle w'_{pi}v'_{pi} \rangle \partial t_{pi}}{\partial r}$, fifteenth $\frac{\beta_i \langle t'_{pi}w'_g \rangle}{\tau_i}$, and seventeenth $\frac{6\beta_i \alpha_{\Sigma i} \langle t'_g w'_{pi} \rangle}{\partial_{pi} c_{pi} \delta_i}$ terms of the right-hand side of the above equation. Rapid growth in the $\langle t'_{pi}w'_{pi} \rangle(r)$ curve in the range $0.045 \text{ m} < r < 0.073 \text{ m}$ is due to the growth in the functions $\langle w'_{pi}v'_{pi} \rangle(r)$, $\langle t'_{pi}w'_g \rangle(r)$, and $\langle t'_g w'_{pi} \rangle(r)$ and the decrease in the dependence $t_{pi}(r)$ in this zone. On the descending portion $0.073 \text{ m} < r$, decrease in the function $\langle t'_{pi}w'_{pi} \rangle(r)$ is caused by the decrease in the tangential Reynolds stress $\langle w'_{pi}v'_{pi} \rangle$ and the mixed correlations $\langle t'_{pi}w'_g \rangle$ and $\langle t'_g w'_{pi} \rangle$ in the interval in question.

Conclusions. The mathematical model given in this work makes it possible to obtain detailed information on the aerodynamic structure, heat exchange, and combustion of the polydisperse ensemble of a coke-ash mixture in different cross sections of the reactor, which can be useful in designing such devices at the stages of engineering and working design.

NOTATION

B , flow rate, kg/sec; C , concentration, kmole/m³; c , heat capacity, kJ/(kg·K); F , force, kg/(sec²·m²); G , generation of turbulent energy of the gas in the wakes of the particles, kg/(sec³·m); g , free-fall acceleration, m/sec²; H , universal gas constant, kJ/(kmole·K); J , coefficient of turbulent diffusion, m²/sec; K , coefficient of restitution; k , kinetic pulsation energy, m²/sec²; L , reaction-rate constant, m/sec; M , number of fractions; m , particle mass, kg; N , frequency of impacts, 1/sec; n , number concentration of particles; P , gas pressure, N/m²; Pr , Prandtl number; Q , thermal effect of the reaction $C + O_2 = CO_2$, kJ/kmole; R , channel radius, m; r, z , radial and longitudinal coordinates, m; S , mass-exchange coefficient, m/sec; t , temperature, °C; u, v , and w , averaged components of the velocity vector, m/sec; U_1, U_2 , and U_3 , coefficients; \mathbf{V} , velocity vector; Z , weight fraction of the component of the gas mixture; α , coefficient of heat exchange between the gas and the particle, kJ/(sec·m²·K); β , true volume concentration of particles; δ , particle diameter, m; ε , pulsation-energy dissipation, m²/sec³; η , kinematic viscosity, m²/sec; μ , molecular weight, kg/kmole; ρ , density, kg/m³; σ , empirical constant; τ , dynamic-relaxation time, sec; ψ_1 and ψ_2 , coefficients, sec⁻¹; ω , parameter. Subscripts and superscripts: a, aerodynamic drag of a particle; ash, ash; col, collisions; g, gas; m, mean value; n, normal; p, particle; t, pulsations; w, channel wall; τ , tangential; $\chi = 1-3$ refer to O₂, CO₂, and N₂; Σ , total (radiant + convective) heat exchange (or the total frequency of collisions due to the random and averaged motion); 0, initial conditions; 1, 2, 3, and 4, fraction numbers of coke particles; ' , pulsation component in time averaging; $\langle \rangle$, time averaging.

REFERENCES

1. A. A. Shraiber, B. B. Rokhman, and V. B. Red'kin, Effect of different factors on coke combustion in a highly concentrated polydisperse ascending flow, *Inzh.-Fiz. Zh.*, **60**, No. 2, 225–230 (1991).
2. B. B. Rokhman and A. A. Shraiber, Mathematical modeling of aerodynamics and physicochemical processes in the freeboard zone of a circulating fluidized bed furnace. 1. Statement of the problem. Basic aerodynamic equations, *Inzh.-Fiz. Zh.*, **65**, No. 5, 521–526 (1993).
3. B. B. Rokhman and A. A. Shraiber, Mathematical modeling of aerodynamics and physicochemical processes in the freeboard zone of a circulating fluidized bed furnace. 2. Interaction of particles (pseudoturbulence), *Inzh.-Fiz. Zh.*, **66**, No. 2, 159–167 (1994).
4. B. B. Rokhman and A. A. Shraiber, Mathematical modeling of the aerodynamics and physicochemical processes in the free board zone of a circulating fluidized bed furnace. IV. Heat and mass transfer and combustion, *Inzh.-Fiz. Zh.*, **67**, Nos. 1–2, 32–38 (1994).

5. A. A. Shraiber, L. B. Gavin, V. A. Naumov, and V. P. Yatsenko, *Turbulent Gas-Suspension Flows* [in Russian], Naukova Dumka, Kiev (1987).
6. B. B. Rokhman, On the equations of transfer of the correlation moments of dispersed phase velocity pulsations on the stabilized portion of an axisymmetric two-phase flow. 1. Equations for second moments. Algebraic relations for third correlations, *Prom. Teplotekh.*, **27**, No. 3, 9–16 (2005).
7. B. B. Rokhman, Two approaches to closing the equations of momentum and heat transfer in turbulent chemically reactive gas-dispersed flows on the stabilized portion of an axisymmetric channel, *Inzh.-Fiz. Zh.*, **80**, No. 6, 90–101 (2007).
8. B. B. Rokhman, Calculation of a turbulent monodisperse flow in an axisymmetric channel, *Inzh.-Fiz. Zh.*, **81**, No. 5, 844–855 (2008).